University of Thi-Qar Journal Vol.12 No.2 June 2017
Web Site: https://jutq.utq.edu.iq/index.php/main
Email: journal@jutq.utq.edu.iq

Scrutiny of the dynamics of quantum dot semiconductor lasers

https://doi.org/10.32792/utq/utj/vol12/2/2

M. O. Oleiwi[1], A.M.Chekheim[2], H. A. Sultan[3] and C. A. Emshary[3]
1 Department of Physics, College of Science, University of Thi-Qar
2 Directorate of Education , Thi-Qar Province
3 Department of Physics, College of Education for Pure Sciences, University of Basrah , Iraq

Abstract:

The present paper introduces a numerical simulation results of the study from semiconductor quantum dot laser via the solution of four-equations model that describe temporal variations of carrier numbers in the wetting layer, N_{wl}, in the two- fold degenerate ground state, N_{GS}, and in the four- fold degenerate excited state, N_{ES}, and the number of photons, S, emitted from the GS. Varieties of dynamics have been seen to occur as a result of the variation of the parameters that appeare in the above mentioned model.

Keywords: Quantum dot semiconductor laser, Ground state, Excited state.

Introduction:

Since the demonstration of a quantum dot (QD) semiconductor laser [1], the search progress in developing lasers based on QDs has been impressive. Because of their fundamentally different physics that stem from zero- dimensional electronic states, QD lasers now surpass the established planner quantum well lasers technology in several respects. These include their minimum threshold current density, the threshold dependence on temperature, and the range of wavelengths obtainable in given strained layer material systems. Since the QDs grow from self- buried heterostructures, they represent a key potential component of future microcavity light emitters

based on oxide- confined vertical cavity surface emitting lasers (VCSELs) [2], photonic band- gap defect lasers [3], and micro- curved resonators [4].

Optimizing the QD characteristics for use as practical, commercial light sources is based on controlling their density, shape and uniformity during epitaxy. In particular the QDs shape and dimensions plays a large role in determining its dynamic response, as well as the temperature sensitivity of the laser's characteristics. Their density, shape and uniformity also establish the optical gain of a QD ensemble. All three physical characteristics can be engineered through the precise deposition conditions in which temperature, growth rate, and material composition are carefully controlled. The variety of heterostructures possible with the increased variety of material choices is being explored in many laboratories. More through experimental trial and error as opposed to theoretical guidance, understanding is being gained as to how strain in both the QD material and adjoining semiconductor heterostructures influence formation and the electronic structure of self-organized QDs.

In this article we present the results of studying the QD lasers output dynamics against the many quantities that appeared in the theoretical model will be detailed in the next section.

Theoretical model:

The numerical model used in this work is based on the work of Yazdani etal [5], Wang etal [6], Darai etal [7] and Grillot et.al. [8] using the carrier dynamics model, see fig. (1).

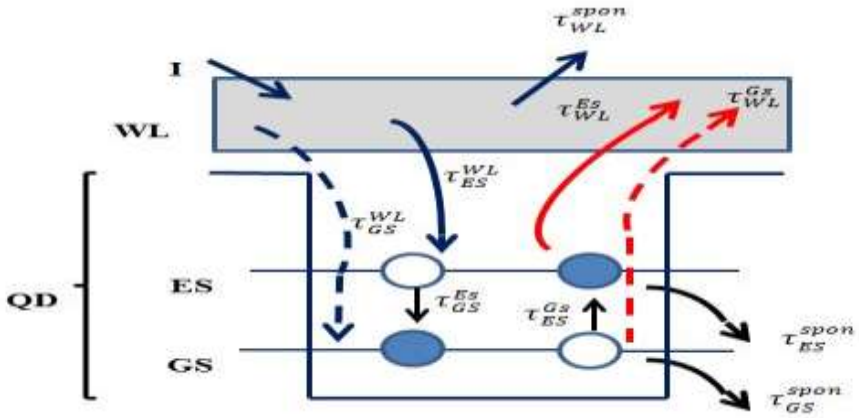

Fig. (1): Carrier dynamics representation with direct (dashed line) relaxation channel schematically in a quantum dot laser.

The QD ensemble includes two energy levels, a two- fold degenerate ground stste (GS) and a four- fold degenerate excited state (ES). Carriers are first injected to the WL before being captured in the ES within a capture time τ_{ES}^{WL} , then the carriers will relax into the GS within a relaxation time τ_{GS}^{ES} .

The carriers can also escape from GS to ES with a time τ_{ES}^{GS} and from ES to WL with a time τ_{WL}^{ES} . Some of the carriers recombine spontaneously with spontaneous emission time τ_{WL}^{Spont} . Based on [5-8] the QD laser dynamics can be described by the following set of equations:

$$\frac{dN_{WL}}{dt} = \frac{I}{q} + \frac{N_{ES}}{\tau_{WL}^{Es}} - \frac{N_{WL}}{\tau_{ES}^{WL}} f_{ES} - \frac{N_{WL}}{\tau_{WL}^{spon}} \quad \ldots. (1)$$

$$\frac{dN_{ES}}{dt} = \frac{N_{WL}}{\tau_{ES}^{WL}} f_{ES} + \frac{N_{GS}}{\tau_{ES}^{Gs}} f_{ES} - \frac{N_{ES}}{\tau_{WL}^{Es}} - \frac{N_{ES}}{\tau_{GS}^{Es}} f_{GS} - \frac{N_{ES}}{\tau_{ES}^{spon}} \quad \ldots. (2)$$

$$\frac{dN_{GS}}{dt} = \frac{N_{ES}}{\tau_{GS}^{ES}} f_{GS} - \frac{N_{GS}}{\tau_{ES}^{Gs}} f_{ES} - \frac{N_{GS}}{\tau_{GS}^{spon}} - \Gamma_P g v_g S \quad \ldots. (3)$$

$$\frac{dS}{dt} = \left(\Gamma_P g v_g - \frac{1}{\tau_p}\right) S + \beta_{sp} \frac{N_{GS}}{\tau_{GS}^{spon}} \quad \ldots. (4)$$

Where, N_{WL}, N_{ES}, and N_{GS} are the carrier numbers in WL, ES and GS respectively. S represents the number of photons emitted from the GS, I is the pump current, q is the electronic charge, $\upsilon_g$is the group velocity, Γ_P is the confinement factor, β_{sp} is the spontaneous emission factor, τ_p is the photon life time, τ_{WL}^{spon}, τ_{ES}^{spon} and τ_{GS}^{spon} are spontaneous emission time of WL, ES and GS respectively. The GS gain, g, can be approximated (for zero gain compression factor) by:

$$g = a_{GS}(\frac{N_{GS}}{V_{QD}} - \frac{N_B}{H}) \quad \text{.... (5)}$$

a_{GS} is the differential gain, N_B is the QD surface density, H is the average height of the QD and V_{QD} is the total volume of the QDs. The blocking factors are f_{GS} and f_{ES}

$$f_{GS} = 1 - \frac{N_{ES}}{2N_B} \quad \text{.... (6)}$$

$$f_{ES} = 1 - \frac{N_{ES}}{4N_B} \quad \text{.... (7)}$$

Simulation results and discussion:

The set of equations (1-4) were numerically solved using the fourth order Runge- Kutta method by Matlab software using the parameters given in Table (1). Fig.(2) reveals the development of the laser signal by solving the related equations for very short time << nanosecond, where the chaotic feature of the spontaneous emission can be easily seen in figures (2 a-c). A great jump in the level of power occurs when the integration time is 0.04 ns (fig. 2d).

Table (1): Numerical used in the simulations

Symbol	Description	Value	Units
N_B	QD surface density	4.3×10^8	cm^{-2}
I/q	ratio of pump current to electronic charge	1×10^{17}	sec^{-1}

τ_{ES}^{WL}	capture time of carriers in ES from WL	14.6×10^{-8}	sec
τ_{GS}^{ES}	relaxation time from ES to GS	5.8×10^{-8}	sec
τ_{ES}^{GS}	escape time from GS to ES	5.8×10^{-8}	sec
τ_{WL}^{ES}	escape time from ES to WL	14.6×10^{-8}	sec
τ_{GS}^{spon}	spontaneous emission time of GS	1200×10^{-8}	sec
τ_{ES}^{spon}	spontaneous emission time of ES	500×10^{-8}	sec
τ_{WL}^{spon}	spontaneous emission time of WL	500×10^{-8}	sec
τ_p	photon life time	5×10^{-15}	sec
υ_g	group velocity	9.435×10^{4}	cm/sec
β_{sp}	spontaneous emission factor	1×10^{-6}	-
Γ_P	confinement factor	0.04	-
H	height of the QD	5×10^{-7}	cm
a_{GS}	differential gain	5×10^{-15}	cm^2
V_{QD}	total volume of the QDs	0.3925×10^{-18}	cm^3

When integration time is ≥ 0.04 ns the relaxation oscillation in the transient region started as can be seen in fig.(2e), which dies out at time > 0.4 ns as can be seen in figs.(2 f-j), as the laser output reach's asteady state.

The relaxation or captured time can affect the laser dynamics. Decreasing the relaxation time, τ_{ES}^{GS} from 5.8×10^{-10} sec to 5.8×10^{-12}sec reduces the number of oscillations in the transient region, decreasing the frequency of oscillation in the same region, and increasing the laser output level for the same total volume of QDs, V_{QD}, (see fig.3).

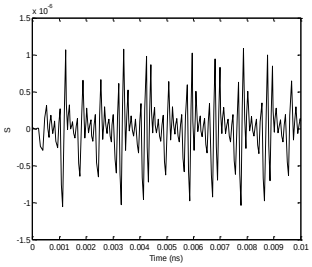
x 10^-6
S
Time (ns)

(a)

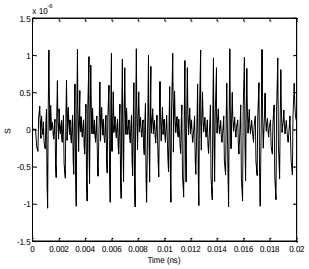
x 10^-6
S
Time (ns)

(b)

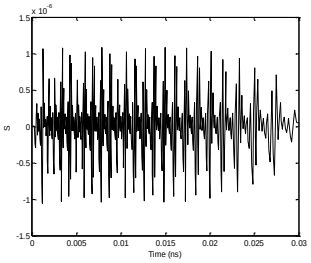
x 10^-6
S
Time (ns)

(c)

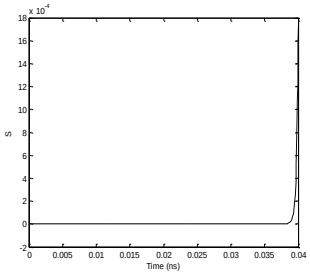
x 10^-4
S
Time (ns)

(d)

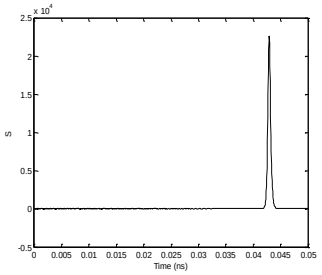
x 10^-4
S
Time (ns)

(e)

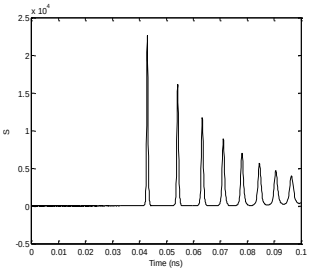
x 10^-4
S
Time (ns)

(f)

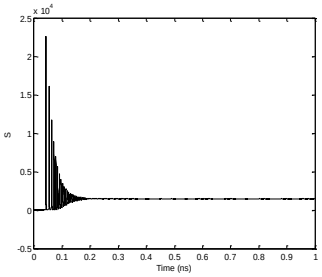
x 10^-4
S
Time (ns)

(g)

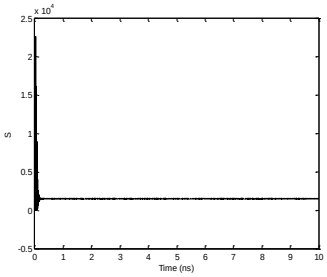
x 10^-4
S
Time (ns)

(h)

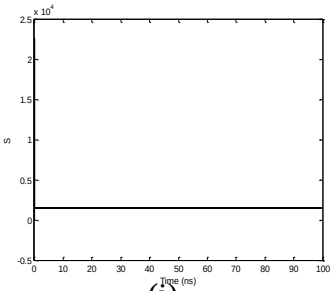
x 10^-4
S
Time (ns)

(i)

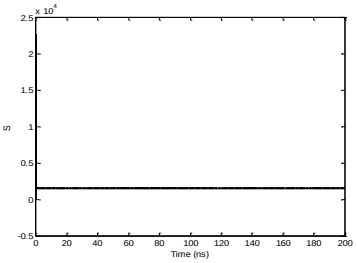
x 10^-4
S
Time (ns)

(j)

Fig. (2): Temporal evolution of the laser signal from QD laser, for the parameters values in table (1)

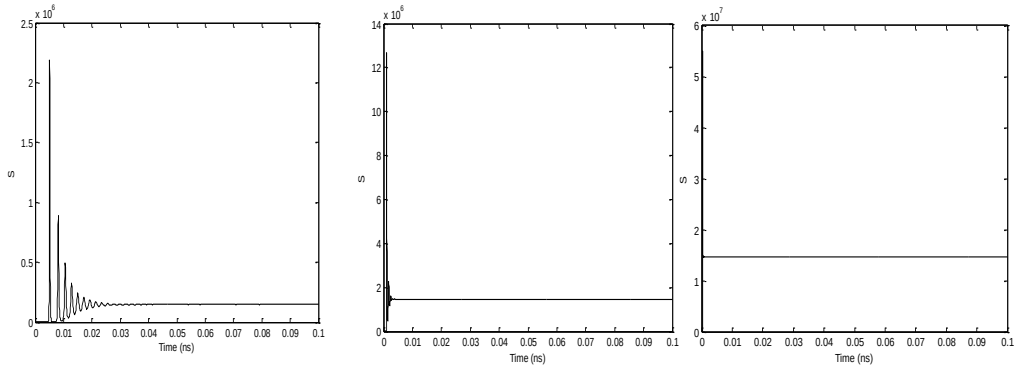

(a) (b) (c)

Fig. (3): Effect of decreasing escape time from ES to GS, τ_{ES}^{GS}on the turn- on dynamics of the QDL: $\tau_{ES}^{GS}(ns) =$ a:0.58, b: 0.058, c: 0.0058.

For the same τ_{ES}^{GS} value and increasing V_{QD} increases the length of the transient region, decreasing its frequency (see fig.4).

Increasing all times, τ_{WL}^{ES} , τ_{ES}^{WL} , τ_{GS}^{spon}, etc vanishes the laser output ending with noisy output overcomed by spontaneous emission only as can be seen in fig. (5).

As the QD surface density,N_B,increases so does the power output of the laser up to $N_B = 10^{11} cm^{-2}$ then the output signal distorted for higher N_Bs, see fig. (6).

When the confinement factor, Γ_P, starts with 0.001 value the output is very low (=0.038) then it increases to 2.5 as Γ_P =0.015 then a large jump occurs when Γ_P =0.018 to 2.4× 10^6 and reaches 7.5 × 10^6 at Γ_P =0.03. The output then increases slowly and reaches constant value as Γ_P varies between 0.04 and 0.1almost reached constant value at Γ_P =0.2, see fig.(7). Through the range of the spontaneous emission factor, β_{sp} , ($10^{-10} - 10^{-1}$) we did not sense clear effect of β_{sp} on the dynamics of the QDL except on the highest

value of the oscillations in the transient region and minimal increasing in the steady state part of the output signal.

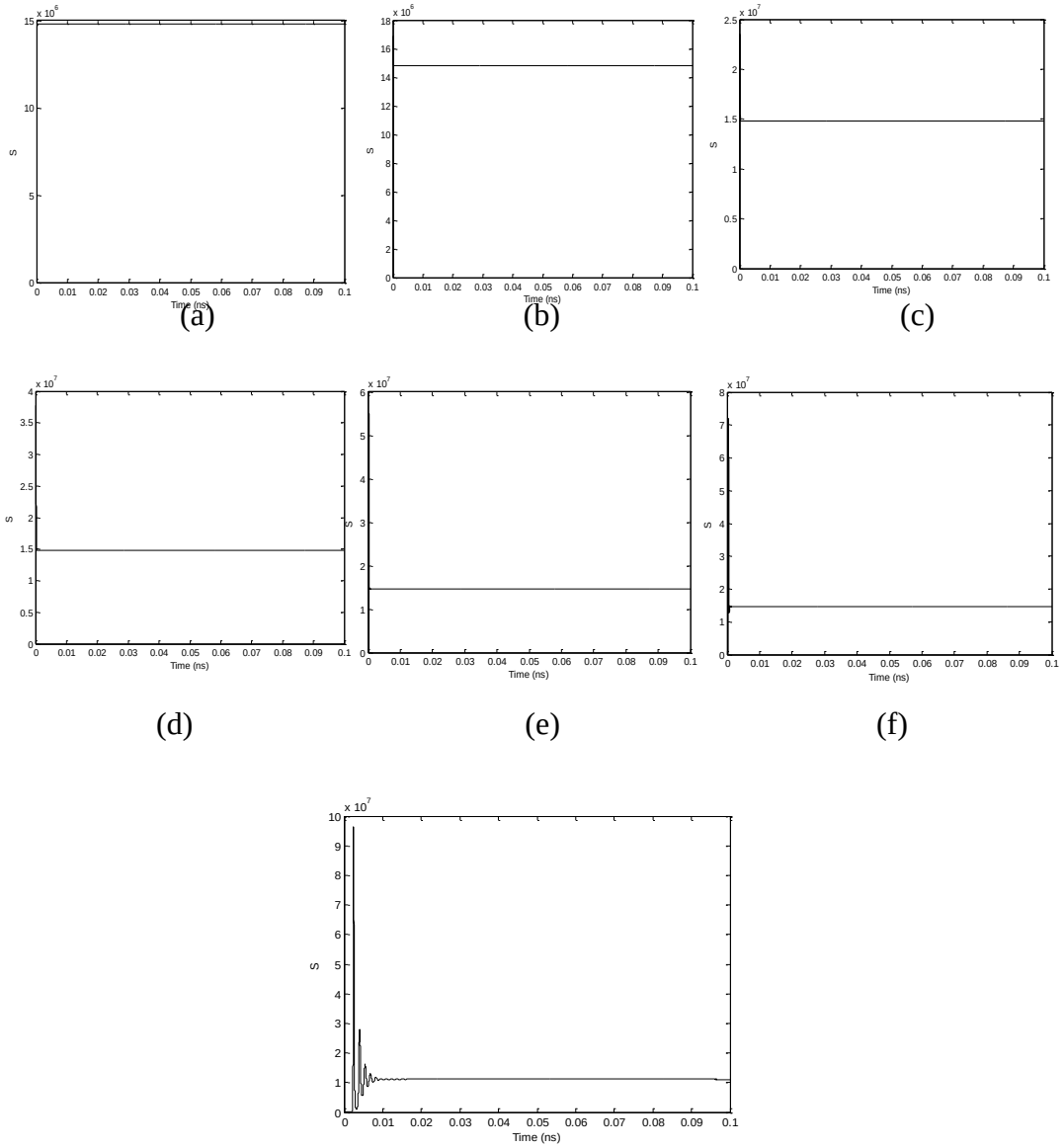

Fig. (4): Effect of total volume of the QDs, V_{QD} on the turn- on dynamics,

for fixed τ_{ES}^{GS} and $V_{QD}(10^{-18}cm^{3})$= a: 0.01652, b: 0.09652, c:0.18652, d: 0.58652, e: 1.58652, f: 3.58652, g: 5.58652.

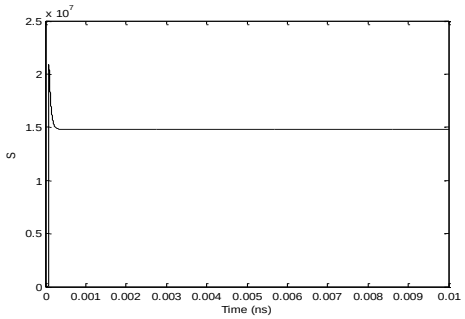

(a)

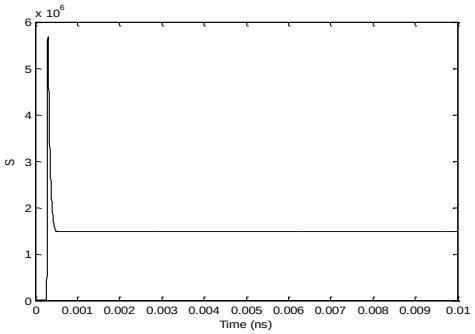

(b)

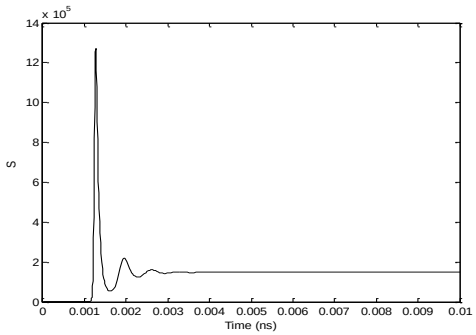

(c)

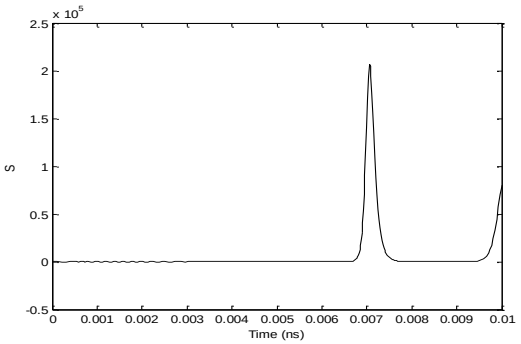

(d)

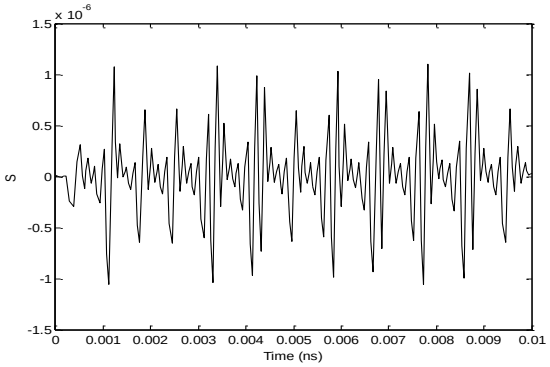

(e)

Fig. (5): Temporal variation of photon density from the QDL using all the parameters in table (1) except: $\tau_{ES}^{GS}(ps) = (a)$: 14.6, (b): 146, (c): 1460, d: 14600, e: 146000.

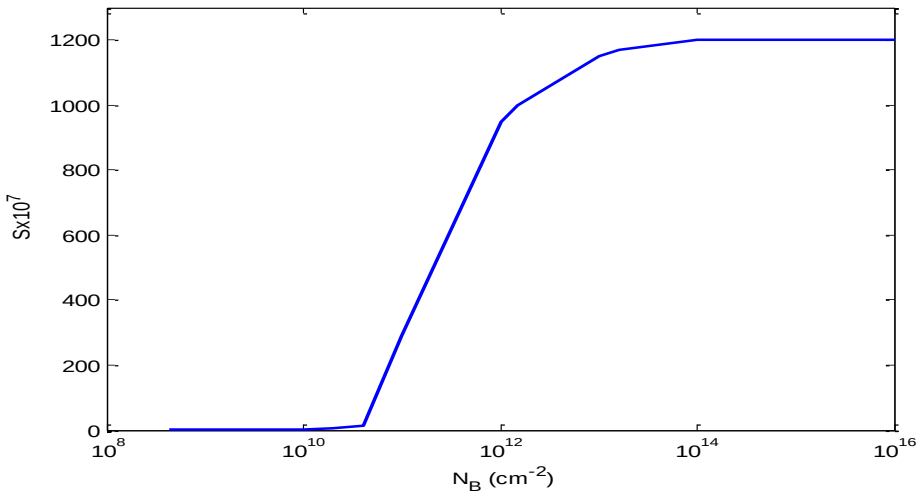

Fig. (6): Variation of the dc-level of the laser output from the QDL against QD surface density, and the rest of parameters values given in table (1).

.

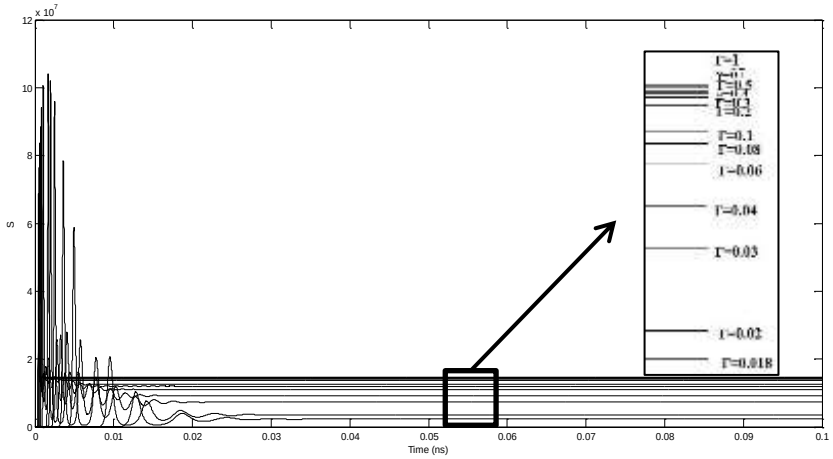

Fig. (7): Laser signal for photon density in QDL for all the parameter values given in table (1) except when Γ_P varied as: a: 0.018, b: 0.02, c:0.03,

d: 0.04, e: 0.06, f: 0.08, g: 0.1, h: 0.2, i: 0.3, j: 0.5, k: 0.7, l: 1.

Very little effect of the variation of beyond the group velocity, $\upsilon_g = 3.39 \times 10^4$ cm/sec as can be seen in fig.(8). The usual laser signal obtained from the QDL appeared when the photon life time $\tau_p = 20 \times 10^{-15}$ sec and as τ_p increased, the transient region shrinks, and disappeared when $\tau_p = 400 \times 10^{-15}$ sec and square signal appeared when $\tau_p = 1350 \times 10^{-15}$ sec. Fig. (9) is the result of increasing τ_p

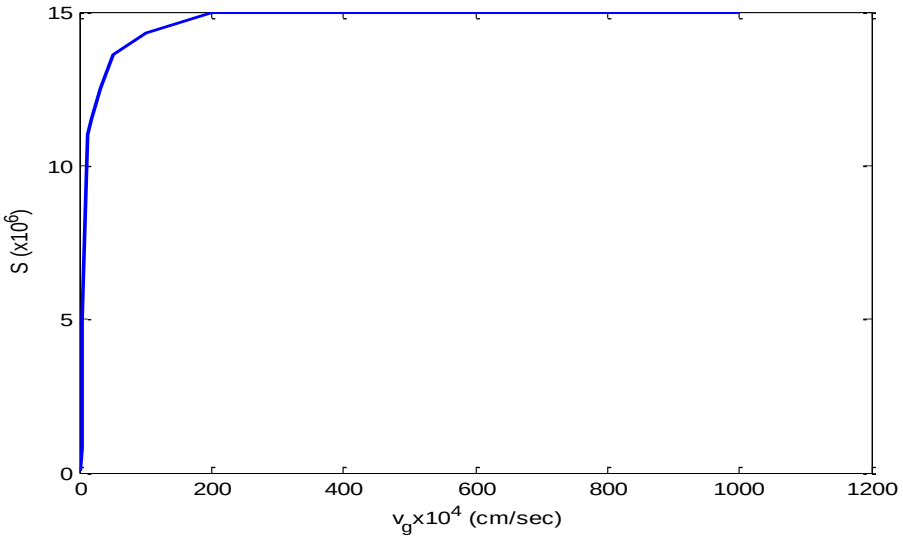

Fig. (8): Variation of the dc level of the photon density, S, using the parameters values given in table (1) and varying the group velocity.

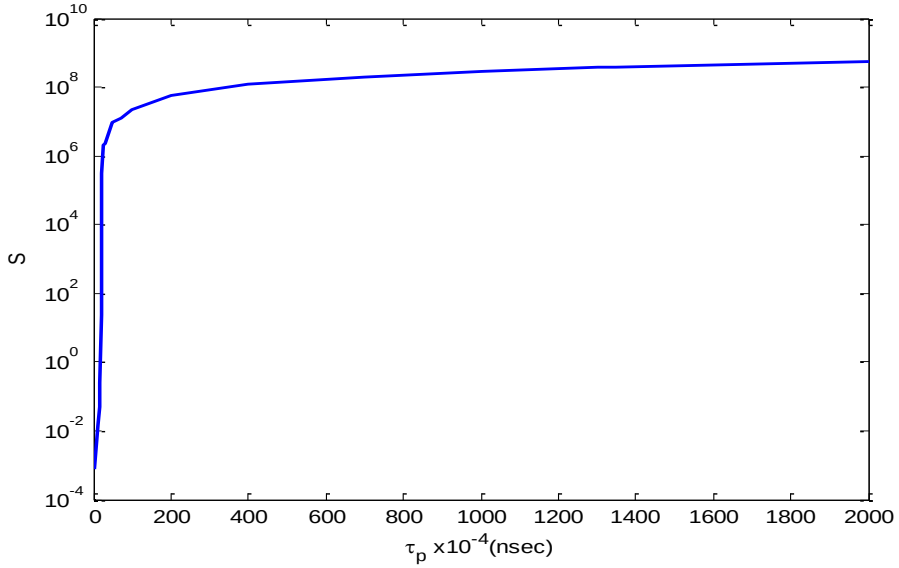

Fig. (9): Variation of the dc level of the photon density, S, of the QDL against photon life time, τ_p,using the parameters values given in table (1).

Conclusions:

According to the obtained results we conclude the following: As increasing the photon life time,τ_p, increases the photons number in the QDL sharply then it reach's saturation. The same behavior occurs for increasing the group velocity, υ_g. Moderate values of the confinement factor, Γ_P push's the QDL to high values of photon number while increasing QD surface density, N_B, slowly increasing the photons number and as the N_B reach's $10^{10}cm^{-2}$ the photons number switch to very high values. The total volume of the QD's, V_{QD}, does not affect the photons number on its own, this is dependent on the escape and capture times, τ_{ES}^{GS}, etc.

References:

1- Zn. I. Alferov, The history and future of semiconductor heterostructures, Semiconductors, 32, 1-14 (1998).

2- P.L. Gourley, Microstructured semiconductor lasers for high- speed information processing, Nature, 371, 571-577 (1999).

3- G. Painter, R. K. Lee, A. Scherer, A. Yariv, J.D. Obrien, P. D. Dapkus and I.Kim, Two dimensional photonic band- gap defect mode laser, Science, 284, 1819 (1999).
4- Q. Xu, D. Fattal and R.G. Beausoleil, Silicon microwing resonators with 1.5 um radius, Optics Express, 16, 4309-4315 (2008).
5- S. Yazdani, E. Rajaei and A. Shafieenezhad, Optimizing InAs/Inp (113)B quantum dot lasers with considering mutual effects of coverage factor and cavity length on two- state lasing, Int. J. Eng. Res., 3, 172-176 (2014).
6- C. Wang, F. Grilllot, and J. Even, Impact of wetting layer and excited state on the modulation response of quantum dot lasers, IEEE. J. Quant. Electron., 48,1144-1150 (2012).
7- A. Daraei, S. M. Izadyar, and N. Chenarani, Simulation and analysis of carrier dynamics in the InAs/GaAs quantum dot laser, based upon rate equations, Opt. Photo.J., 3, 112-116 (2013).
8- F. Grillot, C. Wang, N. A. Naderi, and J. Even, Modulation properties of self- injected quantum dot semiconductor diode lasers, IEEE Sel. Quant. Electron., 19, 1900812 (2013).

تفحص حركيات ليزرات النقطة الكمية

مشتاق عبيد عليوي[1] و علي مهدي جخيم[2] و حسن عبد الله سلطان[3] و جاسب عبد الحسين مشاري[3]
1 قسم الفيزياء , كلية العلوم , جامعة ذي قار
2 مديرية التربية , ذي قار
3 قسم الفيزياء ,كلية التربية للعلوم الصرفة , جامعة البصرة

الخلاصة

في البحث الحالي نقدم نتائج المحاكات العددية لدراسة حركيات ليزر النقطة الكمية عن طريق حل انموذج رياضي يتكون من اربعة معادلات تصف التغيرات الزمنية لعدد الحاملات في منطقة الترطيب وفي الحالة الأرضية ذات الأنحلال الثنائي والحالة المتهيجة ذات الأنحلال الرباعي في

النقطة الكمية واخيراً عدد الفوتونات المنبعثة من الحالة الأرضية . حصل العديد من الحركيات عن طريق تغير العديد من المتغيرات التي يحتويها الأنموذج اعلاه.